Perdigão CFD Grid Study

DTU Vindenergi
E Rapport 2016

Andreas Bechmann

DTU Wind Energy E-0120 (EN)

Marts 2016

DTU Vindenergi
Institut for Vindenergi

Author: Andreas Bechmann

Title: Perdigão CFD Grid Study

Department: DTU Wind Energy

Abstract:
This report is part of the work performed by work package 3 deliverable M12 of the 'New European Wind Atlas' project (FP7-ERANET-2013). The purpose of the deliverable is to list the characteristics of the microscale models from all NEWA partners and document the methodologies used to minimise numerical errors, in particular due to the Computational Fluid Dynamics (CFD) grid of the microscale model. This report documents the work done to minimize the numerical errors of the DTU Wind Energy microscale model 'WAsP CFD'.

Marts 2016

ISSN:
ISBN:
978-87-93278-78-3

Cover:

Pages: 23
Tables: 2
Figures: 13
References: 14

Danmarks Tekniske Universitet
DTU Vindenergi
Frederiksborgvej 399
4000 Roskilde
Denmark
Tel. +45 4677 5024
andh@dtu.dk
www.vindenergi.dtu.dk

Content

1. Introduction

In this report, we conduct a grid independence study of microscale Computational Fluid Dynamics (CFD) simulations of the Perdigão site in Portugal. The investigation is part of the New European Wind Atlas (NEWA) project and is conducted to evaluate the numeric requirements for microscale CFD models used for wind resource assessment. Running CFD models on coarse grids can cause significant erroneous results when assessing a wind farm power potential. This study can hopefully guide to choose a proper microscale CFD setup for the NEWA project.

In general, CFD grid independence studies access the accuracy of the numerical solution to a particular problem posed by the grid and boundary conditions used. Therefore, it is important that the CFD problems investigated in this report be similar to the CFD problems of the NEWA project. However, since these are unknown, we study the accuracy of the WAsP-CFD approach Troen et al. (2014); Bechmann (2013) and assume it comparable to the method selected in the NEWA project. We chose the WAsP-CFD approach because of its well-defined methodology for generating grids and boundary conditions that allow for a systematic and objective grid independence analysis.

Bechmann et al. (2011) made a comparison of fifty-seven microscale models ability to capture the flow around the Bolund Hill. In the Bolund comparison the total error of the microscale models was compared i.e. the numerical, modeling and other errors were combined. This report tries to make an analysis of the most important numerical errors separately.

2. Perdigão

The Perdigão site, located in the centre of Portugal, contains two approximately *500* m high parallel ridges with a distance of about *1.2* km. The ridges are about *4* km long and have northwest-southeast orientation. A *2* MW Enercon E-82 wind turbine (WT) with *82* m hub-height and a *20* m tall meteorological mast (MET) are located on the western ridge at position (*607587.0; 4396060.0*) and (*608384.7; 4395088.0*) respectively (*UTM WGS 1984 Zone 29*), see figure *1*.

A *6*x*8* km area high-resolution terrain height vector map was combined with SRTM data to make a *50*x*50* km orography map of Perdigão and its environs. Ground roughness was determined from aerial laser scanning performed by Niras in April 2015. Based on the method described by Boudreault (2015) the tree heights was extracted from the laser scanning and was converted to roughness by assuming a roughness length equal to one tenth of the tree height. Since the aerial scans only cover the two ridges a roughness length of 10 cm is assumed for the rest of the area, giving roughness values between *0.1* and *2.3* m. A detailed description of the site and a WindScanner field campaign performed at Perdigão in the summer of 2015 can be found in Vasiljevic (2016).

2.1 Reference roughness and terrain height

To define reference conditions for the CFD grid independency study a target site is first defined. It is inside this area that we explore the effect of changing CFD resolution. In figure *2* the *1.5*x*1.5* km target site is shown. Its centre is located at (*608000.0; 4396400*) and has been chosen so that both the WT position and the flow between the two ridges can be examined. We want the target site to be relatively small so that the reference conditions are applicable to the whole area.

Figure 1: Overview of the Perdigão site showing the WT and MET positions on the western ridge (picture from Google Earth)

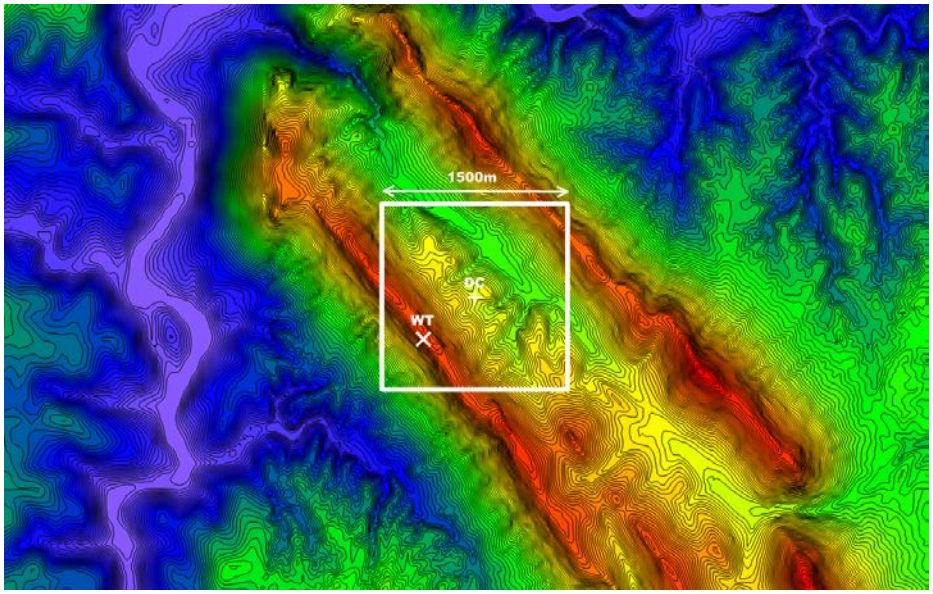

Figure 2: A close-up view the orography map used for CFD simulations. The figure shows the turbine position (WT) and the domain centre (DC)

The reference conditions in the direction in question are determined by the reference roughness, z_{0ref}, also called the "distant roughness" or mesoscale roughness. For the CFD simulations, it is used when specifying the logarithmic inlet conditions and when calculating speed-up ratios (see *eq. 4*). A speed-up of, say, *5* %, means that for the wind direction examined the topography induces an increase of the wind speed of 5% compared to flat terrain with the same constant roughness. As roughness beyond a certain equilibrium distance has no effect on the wind at the target site, the reference roughness includes mainly the terrain roughness within that equilibrium distance (L_e= *9* km used here). Roughness beyond the equilibrium distance is allowed only to be included with a tiny weight, a weight that is decreasing with distance. Reference roughness is further described in section *8.3* of the European wind atlas of Troen and Petersen (1989).

The reference terrain height, z_{ref}, is the "distance terrain height" in the direction of the sector in question. The CFD-model "flattens" the terrain toward this reference height and applies boundary conditions by the reference roughness. For each direction, the orography is flattened using the following blending function,

$$z_{CFD} = (1-\alpha)z + \alpha z_{ref}$$
$$\alpha = \tanh\left(\left(\frac{d}{L_e}\right)^{\beta}\right)$$

where z_{CFD} is the resulting terrain height used for the CFD simulations, β=*0.45* and d is the distance from domain centre. The function is illustrated in figure *3*. As seen, the target zone that extends *750*m from domain centre is not affected by the terrain flattening. At a distance of *2* km the blending function is only α=*0.01* and at *4* km it is α=*0.08*. For the present simulations, the reference terrain height for each direction is found at a distance of 13 km from the domain centre. For the Perdigão simulations, the reference roughness lengths and terrain heights are given in Table *1* have been used. Figure *4* show the orography before and after terrain flattening. A benefit of the far-field flattening is that terrain generated wakes from the CFD

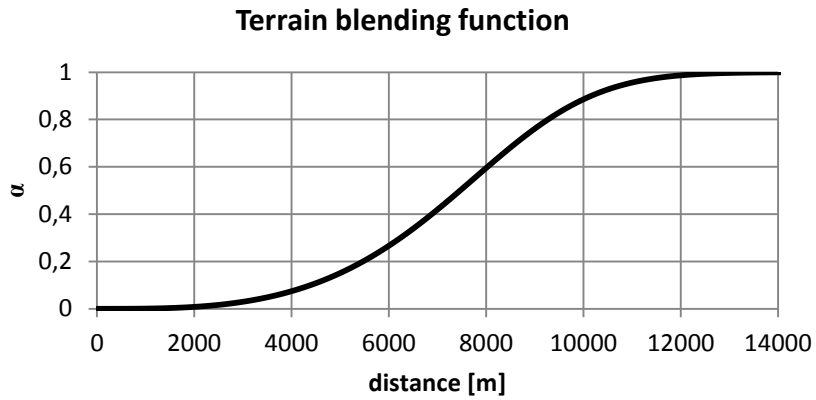

Figure 3: The Blending function used to flatten the far-field terrain for the CFD simulation

simulations have room to recover before reaching the outlet of the domain - this helps convergence of the CFD simulations.

Table 1: reference terrain height and roughness for different direction used for CFD simulations

Dir	***0***	***10***	***20***	***30***	***40***	***50***	***60***	***70***	***80***	***90***	***100***	***110***
z_{ref} [m]	*270.9*	*297.6*	*314.3*	*327.0*	*301.4*	*311.8*	*375.1*	*365.4*	*336.0*	*167.8*	*119.3*	*130.2*
z_{0ref} [m]	*0.108*	*0.109*	*0.102*	*0.111*	*0.108*	*0.110*	*0.109*	*0.103*	*0.108*	*0.115*	*0.122*	*0.113*

Dir	***120***	***130***	***140***	***150***	***160***	***170***	***180***	***190***	***200***	***210***	***220***	***230***
z_{ref} [m]	*193.6*	*169.3*	*118.1*	*273.5*	*157.1*	*105.7*	*175.1*	*255.7*	*184.3*	*190.5*	*197.8*	*216.2*
z_{0ref} [m]	*0.117*	*0.115*	*0.110*	*0.114*	*0.113*	*0.112*	*0.112*	*0.104*	*0.104*	*0.108*	*0.108*	*0.114*

Dir	***240***	***250***	***260***	***270***	***280***	***290***	***300***	***310***	***320***	***330***	***340***	***350***
z_{ref} [m]	*196.9*	*264.9*	*322.4*	*335.4*	*398.3*	*372.1*	*460.0*	*494.9*	*481.6*	*396.3*	*417.2*	*297.7*
z_{0ref} [m]	*0.113*	*0.106*	*0.110*	*0.114*	*0.111*	*0.109*	*0.113*	*0.104*	*0.104*	*0.107*	*0.102*	*0.105*

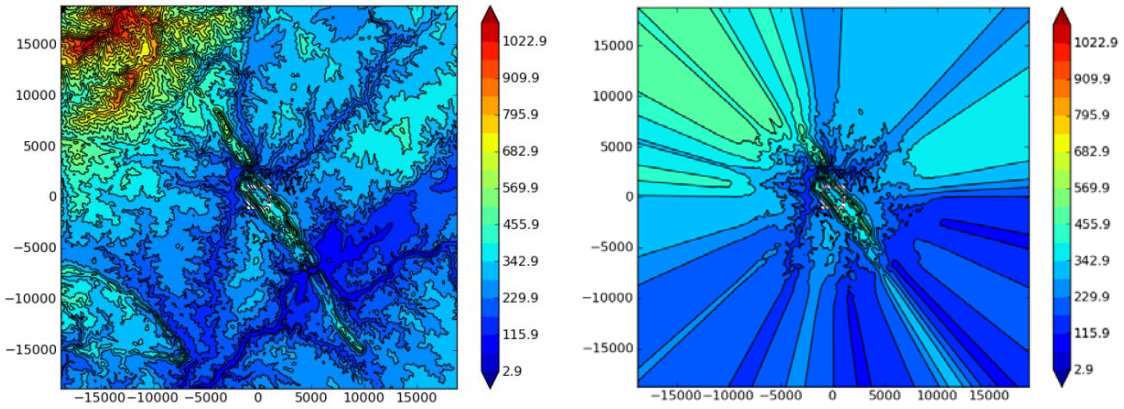

Figure 4: The figure show how the far-field terrain for each direction is flattened toward the reference terrain height. The resulting orography map is used to generate the CFD grid. Left: the original orography map. Right: the flattened orography map.

3. CFD Setup

We want to investigate how the accuracy CFD solution depends on the resolution of the numerical grid. This is in principal done by comparing the solution of a high-resolution grid to that of a lower resolution. While this may seem straightforward, results of grid independence studies are influenced by the CFD setup. Results can vary between grids of equal resolution, can vary due to the wind conditions or directions simulated and vary between CFD solvers because of differences in discretization schemes, turbulence model, etc. The possibilities are endless; here we have chosen only a few.

A high-resolution CFD grid is first made specifically for the CFD solver used, EllipSys3D Michelsen (1992, 1994), Sørensen (1995). EllipSys3D requires a block-structured grid that can be difficult to make but once made; it can naturally be coarsened and provide results for a grid independence test. A polar grid structure is chosen so that any wind direction can be simulated and its influence investigated. Finally, every simulation is repeated with three discretization schemes, a third, second and first order and results compared

3.1 CFD grid

Having flattened the far-field terrain the computational grid can be generated. Since the CFD-model uses terrain-following coordinates, it is possible for the lower boundary of the computational grid to follow the orography. In this work a high-resolution zooming polar grid is used. It consists of a central *3*x*3*km part with high grid resolution and an outer *30*km diameter polar part where the grid resolution gradually coarsens. Instead of projecting the grid vertically when generating the surface grid, true surface projection is used to allow enough resolution even in areas of very steep terrain. The grid resolution in a direction following the terrain (even e.g. vertically-aligned cliff faces) is *10*m in the *3*x*3*km central part. An example of the lower boundary of the zooming grid is illustrated in figure *5*.

To generate the 3D grid, the hyperbolic grid generator HypGrid3D Sørensen (1998) is used. Due to high-velocity gradients the near-wall, the grid cells are only *5*cm tall near the ground but gradually coarsens with height until the top of the domain is reached at about *9700*m Pedersen (2010). The vast domain height has been selected to minimize the effect of blockage of the domain boundaries. *144* grid points are used in the vertical direction and about *90* of these are employed in the first *300*m, giving a low vertical resolution of about *3.4*m in this region. Since the CFD-model uses a block-structured grid arrangement, the whole domain is divided into *180* blocks each of 48^3 cells or about *20* million cells in total. The grid is similar to the mesh used in WAsP-CFD but has a *10*m resolution instead of *20*m.

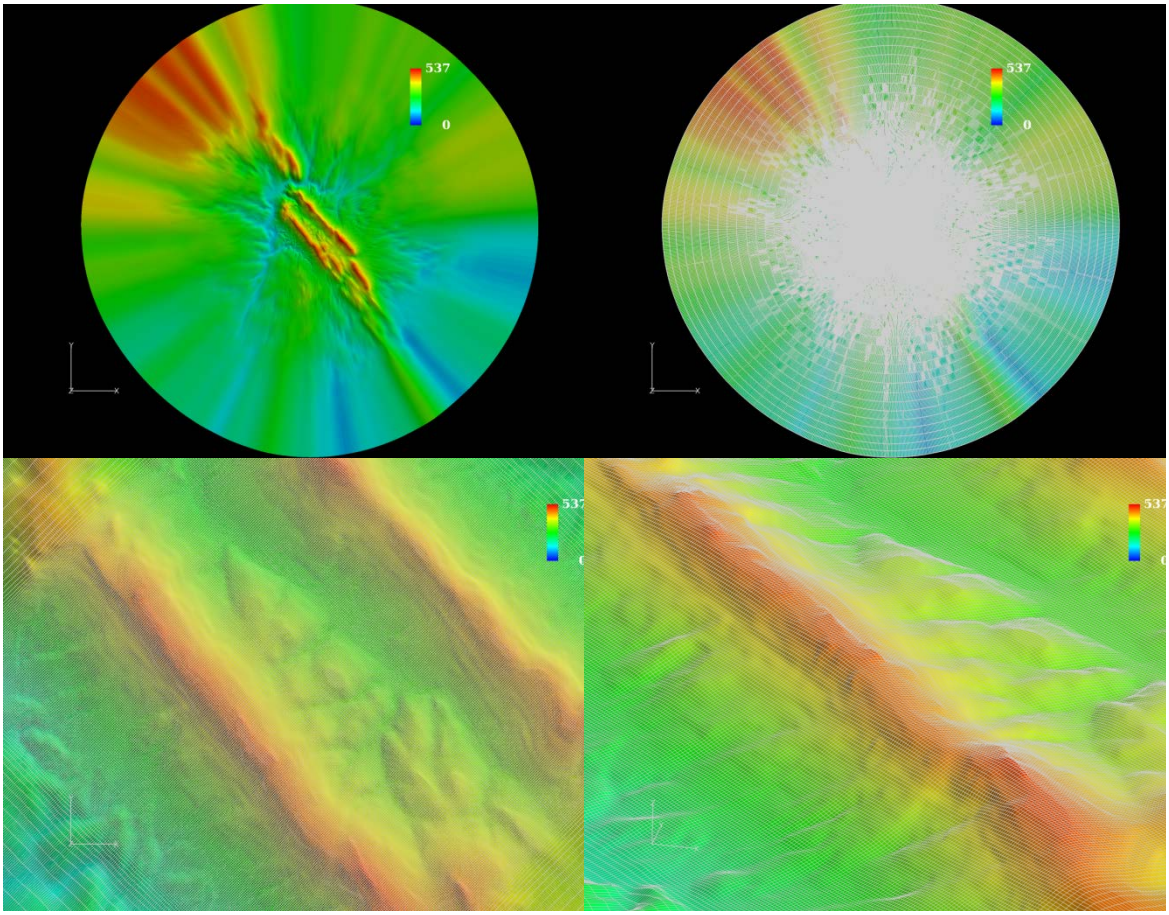

Figure 5: The 30km diameter section of the Perdigão site is shown in the upper left-hand corner of the figure while the surface grid is illustrated in the upper right-hand. The lower pictures show a closer view of the target area (left) and the western ridge (right)

3.2 CFD model

In this report, all CFD simulations are performed with the Ellipsys3D code of Sørensen (1995) and Michelsen (1992, 1994), which is a general-purpose flow solver used for many applications within wind energy. EllipSys3D is a multi-block finite-volume discretization of the incompressible Navier-Stokes equations in general curvilinear coordinates. The user can choose among different discretization schemes for the convective terms, all implemented using the deferred correction approach first suggested by Khosla and Rubin (1974). WAsP-CFD uses a third order scheme (QUICK) to retain high accuracy, but in this work, we will also investigate the second order (SUDS) and first order upwind schemes (UDS) often used in the wind industry. Central differences are used for the remaining terms of the Navier-Stokes equations.

EllipSys3D is parallelized with MPI for execution on distributed memory machines, using a non-overlapping domain decomposition technique and uses a multi-level grid sequence in steady-state computations to further accelerate computations. The parallelization allows for an efficient use of large computer clusters and consequently calculations on large, high-resolution grids, but the multi-level grid sequence has the added benefit of automatically making a grid independence test since EllipSys3D produces a result on each of the differently resolved grid levels. For grid independency tests one high-resolution grid is generated, and its solution (level

1) can be compared to the automatic solutions from a two times coarser grid (level 2), four times coarser grid (level 3) and eight times coarser grid (level 4).

When calculating the wind resources following the European wind atlas concept, the CFD model is only accounting for the atmospheric micro-scales scales, i.e. the near-surface wind with horizontal scales typically ranging from a few kilometres down to a few meters. Coriolis effects tend to act on longer scales and are therefore neglected. The effect of stability is assumed to be small perturbations to the primary neutral state and is also omitted from the CFD simulations. Due to the assumption of neutral stability and the omission of Coriolis effects, the modelled wind becomes Reynolds number independent, which simplifies the grid independency study since we can compare speed-up ratios instead of wind speed.

In this work, we solve the Reynolds Averaged Navier-Stokes (RANS) equations, and the numerical solution is only stopped when all variable residuals are below $1*10^{-5}$. It is important to ensure fully converged solutions for the grid independency study to be accurate. Turbulence is modeled using the two-equation *k-ε* of Launder and Spalding (1974), with fixed model constants calibrated for atmospheric flows.

Table 2: k-ε model constants used for all simulation

C_μ	κ	σ_k	σ_ε	$C_{\varepsilon 1}$	$C_{\varepsilon 2}$
0.052	*0.40*	*1.00*	*1.30*	*1.38*	*1.92*

3.3 Boundary conditions

Since the flow considered is treated as neutrally stratified and Coriolis forcing is neglected; the flow is Reynolds-number independent. The CFD results are therefore only dependent on the inflow direction and on the inflow profiles that are specified as a function of a far-field surface roughness (see *Table 1*).

The Logarithmic equilibrium profiles for the horizontal wind speed, u_0, turbulent kinetic energy, *k*, and the dissipation, ε, are used to specify the inflow conditions (Dirichlet conditions),

$$u_0 = \frac{u_f}{\kappa} ln\left(\frac{z+z_0}{z_0}\right) \qquad \textit{eq. 1}$$

$$k = \frac{{u_f}^2}{{C_\mu}^{1/2}} \qquad \textit{eq. 2}$$

$$\varepsilon = \frac{{u_f}^3}{\kappa z} \qquad \textit{eq. 3}$$

Outlet conditions are common Neuman boundary conditions. To be able to run different wind directions, each simulation specifies outlet conditions for 70 degrees of the downwind boundary while the rest of the horizontal boundary (290 degrees) is set as an inlet. Inlet conditions are also used at the top of the domain.

A wall function is used to model the effect of ground roughness. For EllipSys3D, the above described Logarithmic equilibrium profiles are used to derive the wall-function, see Sørensen (1995) and Sørensen et al. (2007b). As seen in eq. 1 the wall is placed on top of the roughness elements (u = 0 for z=0) and is consequently displaced by the roughness length. This has been done to avoid a minimum height restriction of the first computational cell, and EllipSys3D can thereby resolve significant near-wall velocity gradients using shallow (high aspect ratio) computational cells.

3.4 Simulated case

To perform the grid independency test, we perform a number of simulations and for each compare the results of the different grid levels (see *section 3.2*). Even though the CFD-model calculates velocity perturbations (speed-up) and turnings at all grid points, only the results from the *1.5*x*1.5*km target site is investigated. We use the horizontal grid resolution of the target site to label the results i.e. *10*m, *20*m, *40*m and *80*m for grid level *1, 2, 3* and *4* respectively.

In complex terrain large changes in wind speed can occur for small changes in wind direction, and this affects the grid independence test. Some wind directions will have larger numerical errors than others. Because of this, every 10^o have been simulated leading to *36* wind directions, which allows examining not only the mean error but also spread. To investigate the effect of the discretization scheme, each direction is repeated three times using the QUICK, SUDS and UDS schemes described in *section 3.2*. This leads to a total of *432* cases (*36* directions, *3* discretization schemes and *4* grid levels). For each instance, the fractional speed-up is calculated,

$$\Delta S = \frac{u}{u_0} \qquad \textit{eq. 4}$$

where u is the simulated wind speed and u_0 is the reference wind speed (*eq. 1*) at the same height above ground. Also, a speed error is defined,

$$\varepsilon = \left(\Delta S - \Delta S_{Q1}\right) * 100\% \qquad \textit{eq. 5}$$

where ΔS_{Q1} is the speedup of grid level 1 of the simulation performed with the QUICK scheme.

4. Results

Figure 6 shows the mean absolute speed error in the target site for the 36 simulated directions at 5, 48 and 150m above ground for the different grid resolution and each discretization schemes. In the appendix the same results are found for each 30-degree sector i.e. these are only the average of 3 simulated directions.

Figure 6 shows that the numerical error increases for increasing resolution and for lower order discretization scheme. It is also seen that the error is larger close to the ground. As an example, the mean error at *150*m *a*bove ground for *20*m grid resolution is *1.4*%, *3.4*% and *7.1*% for the QUICK, SUDS and UDS scheme respectively. The numerical error is, therefore, more than 2 times higher when using a second order scheme and five times higher when using a first order scheme compared to the third order scheme. The same kind of increase in error is seen when the grid resolution is coarsened i.e. 1.4%, 3.3% and 6.1% error for *20*m, *40*m and *80*m respectively.

Figure 7 shows the average absolute speed error at the WT-site. The results are an average of 36 simulations extracted at 48, 65, 80, 100, 120, 150m above ground. For 20m grid resolution the mean absolute speed error is found to be 0.8%, 2.1% and 4.2% for the three discretization schemes. The average error is, therefore, smaller at the WT-site compared to the average for the whole target site but still not negligible. In broad strokes the tendency that the error is doubled each time that the order of the discretization is schemes lowered or the resolution is doubled is repeated at the WT-site. Sector averaged results for the WT-site can be found in the appendix

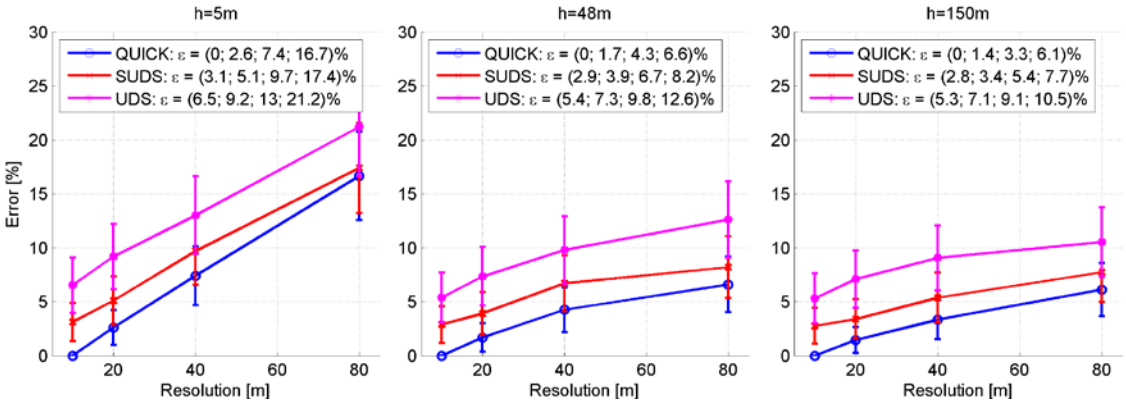

Figure 6: Mean absolute speed error as a function of grid resolution in the target site for 5 m (left), 48 m (middle) and 150 m (right) above ground. The results are the mean of 36 CFD simulations using the QUICK (blue), SUDS (red) and UDS (pink) discretization schemes.

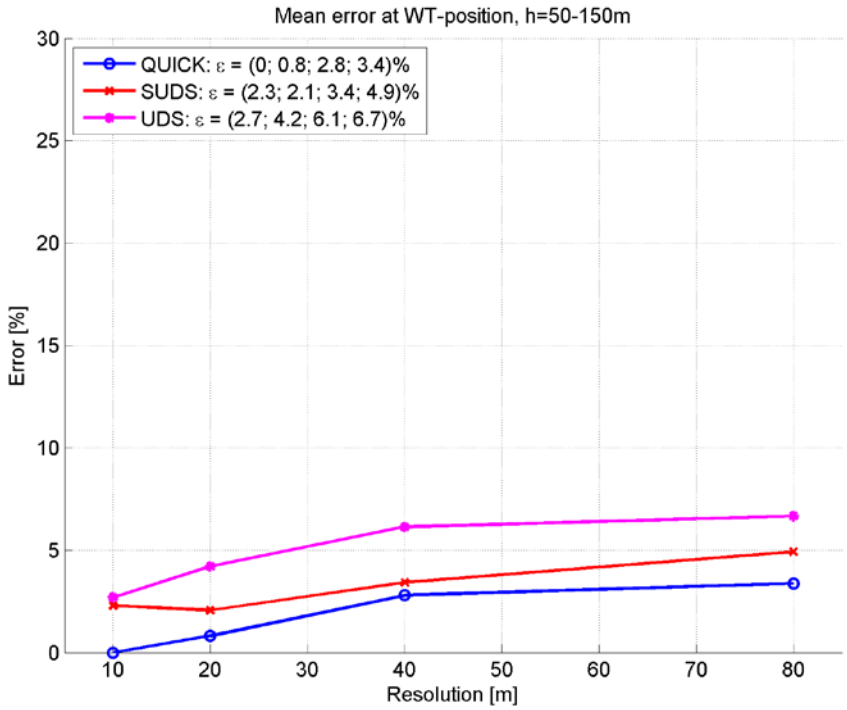

Figure 7: Mean absolute speed error as a function of grid resolution at the WT-position. The results are the mean of 36 CFD simulations, extracted at 48, 65, 80, 100, 120, 150m above ground using the QUICK (blue), SUDS (red) and UDS (pink) discretization schemes respectively.

5. Summary and Conclusions

Despite the use of proper numerical techniques, CFD results will always have a little numerical uncertainty. The right balance between computational cost and model resolution is hard to find and must be weighed against other forms of uncertainties in the model chain.

Results show a tendency that the mean numerical error in the target area approximately doubles with double the resolution and doubles for each order that the discretization scheme of the convective term is lowered. Proper discretization of the flow equations is therefore just as important as the resolution of the computational grid. As an example, an *80* m resolution simulation that uses the third order QUICK is more accurate than a 20m resolution simulation that uses first order UDS. In general, if one is not very careful with the choice of both discretization scheme and grid resolution the numerical errors quickly add up, making the CFD results useless for wind resource assessment.

When looking at the errors only at the single WT-position (*figure 7*), results are less clear. As expected, that the error at the turbine position (hill top) is smaller than in the target area (include wake regions), but other observations can also be made:

1. As the simulations coarsen (resolution and discretization), the error seems to reach a plateau where it grows less rapidly.
2. The *10*m resolved SUDS simulation has larger errors than the *20*m resolved SUDS simulation.

These examples illustrate the difficulties in doing grid independence studies.

1. If the best-resolved CFD simulation used for the grid independency study is too coarse, the numerical error will be underestimated. As an example, the error difference between the *20* m and *80*m resolved UDS simulations is only 2.5%. However, the error for the 80m resolved simulation is much larger. Using the *10*m QUICK simulation as a reference; the error is found to be 6.7%; though even this is too low as the *10*m QUICK also has numerical errors.
2. Many simulations have to be performed and compared for many positions for the results to be statistically significant.
3. The reduction in error is lower than expected from the formal second order accuracy of the applied code. This indicates that the finest mesh used in this report have terrain features that are not resolved. Similar conclusion was found by Sørensen et al. (2012) using a grid of *2.5*m resolution

WAsP-CFD has been designed primarily to be used for wind resource estimation in complex terrain, where even small errors can impact the success of a wind farm project. During the design of WAsP-CFD, the focus has therefore been on achieving numerical accuracy, and a solution that leaned toward a high resolution (*20* m) and a high order discretization scheme (QUICK) was chosen. As seen in the result section, this lead to a numerical error of about 0.7% at the WT position and *1.4-1.7*% in the mean for the target area of the Perdigão site (assuming zero error for the *10*m QUICK simulations).

The presented speed-up results are a measure of the error when using the inlet as a reference (distance from inlet to target area is about *15*km). The error will be smaller if a nearby mast position is used as a reference. However, for most results, it is important that CFD model accurately represent the prescribed boundary conditions. Therefore, the inlet is used as a reference for the presented results.

References

Bechmann, A., Sørensen, N.N., Berg, J., Mann, J. and Réthoré, P.-E. 2011: The Bolund Experiment, Part II: Blind Comparison of Microscale Flow Models. *Boundary-Layer Meteorol*. **141**, 245-271.

Bechmann, A., 2013: *WAsP CFD*. [*ONLINE*] Available at: http://www.wasp.dk/waspcfd.

Boudreault, L-É., A. Bechmann, L. Tarvainen, L. Klemedtsson, L. Shendryk, E. Dellwik, 2015: A LiDAR method of canopy structure retrieval for wind modeling of heterogeneous forests. *Agricultural and Forest Meteorology*, **201**, 86-97.

Khosla P. and Rubin S., 1974: A diagonally dominant second-order accurate implicit scheme. *Comput Fluid*, **2**, 207—289

Launder, B.E. and D.B. Spalding, 1974: The numerical computation of turbulent flows. *Comput. Meths. Appl. Mech. Eng.*, **3**, 269–289.

Michelsen J.A., 1992: Basis3D – a platform for development of multiblock PDE solvers. *Technical report AFM 92-05*, Technical University of Denmark

Michelsen J.A., 1994: Block structured multigrid solution of 2D and 3D elliptic PDE solvers. *Technical report AFM 94-06*, Technical University of Denmark

Pedersen J.P., 2010: Improved inlet conditions for terrain CFD. *Master thesis*. Risø, National Loboratory for Sustainable Energy, Technical University of Denmark.

Sørensen, N. N., 1995: General purpose flow solver applied to flow over hills. *Technical report, Risø*. URL http://www.citeulike.org/user/pire_1024/article/5890204.

Sørensen, N. N., 1998: HypGrid2D a 2-D mesh generator. *Technical report, Risø DTU, Roskilde, Denmark*. URL 130.226.56.153/rispubl/VEA/veapdf/ris-r-1035.pdf.

Sørensen, N. N., A. Bechmann, J. Johansen, L. Myllerup, P. Botha, S. Vinther, and B. S. Nielsen, 2007: Identification of severe wind conditions using a Reynolds Averaged Navier-Stokes solver. *Journal of Physics: Conference Series*, 75:012053, July 2007a. ISSN 1742-6596. doi:10.1088/1742-6596/75/1/012053.

Sørensen, N. N., A. Bechmann, P-E. Réthoré, D. Cavar, M. C. Kelly, I. Troen, 2012: How fine is fine enough when doing CFD terrain simulations. Proceedings of EWEA 2012 – European Wind Energy Conference & Exhibition. European Energy Association (EWEA).

Troen, I. and E. L. Petersen, 1989: European Wind Atlas. *ISBN 87-550-1482-8*, Risø National Laboratory, Roskilde. 656 pp.

Troen, I., Bechmann, A., Kelly, M. C., Sørensen, N. N., Réthoré, P-E., Cavar, D., & Ejsing Jørgensen, H., 2014: Complex terrain wind resource estimation with the wind-atlas method: Prediction errors using linearized and nonlinear CFD micro-scale models. In *Proceedings of EWEA 2014.* European Wind Energy Association (EWEA).

Vasiljevic, N., Palma, J.L., Angleou, N., Matos, J.C., Lea, G., Mann, J., Courntey, M., and Ribeiro, L.F., 2016: Perdigão 2015: Windscanner Field Campaign. *Submitted to journal*

6. Appendix

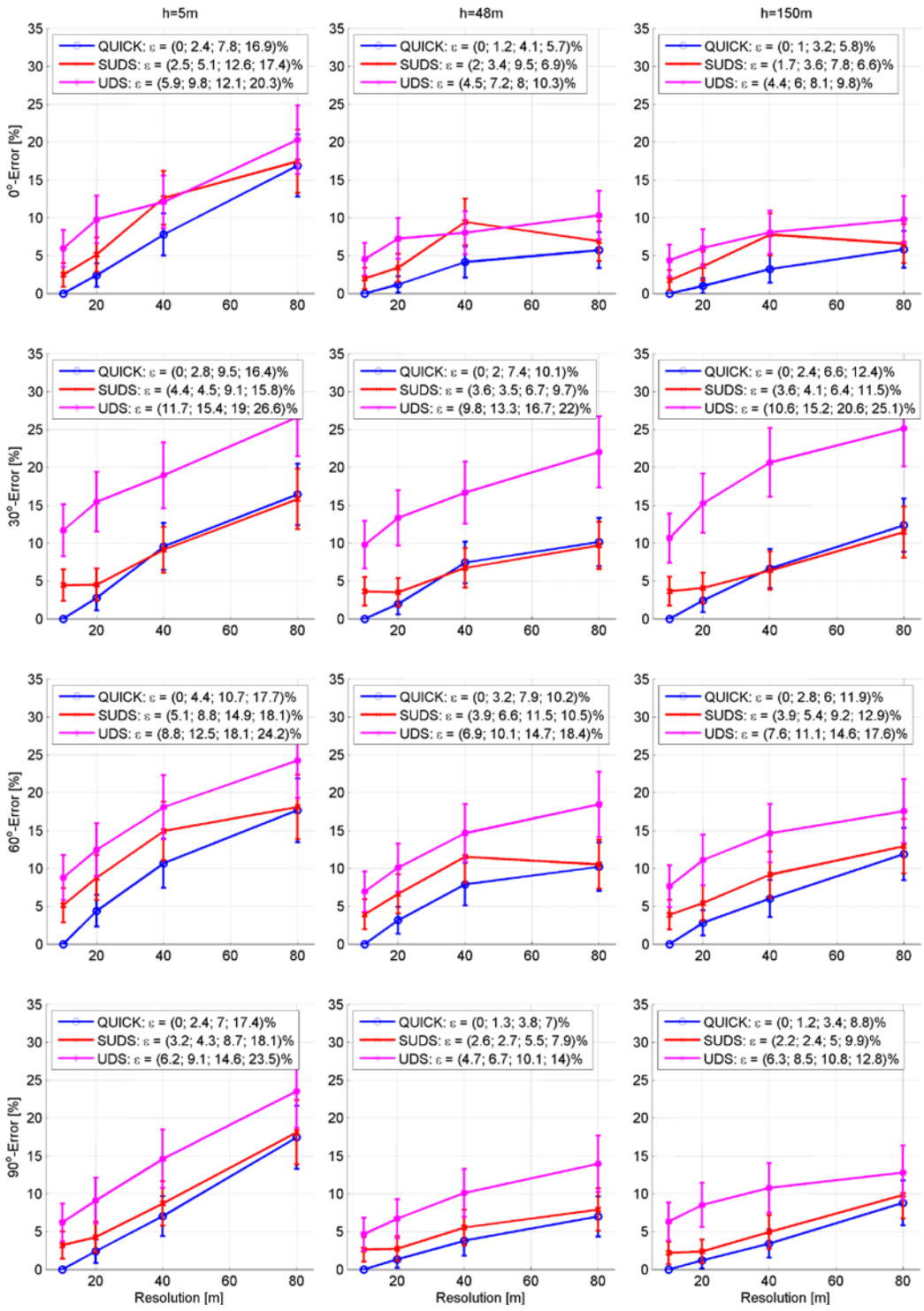

Mean Speed error in the target area for the 0-90 degree wind direction

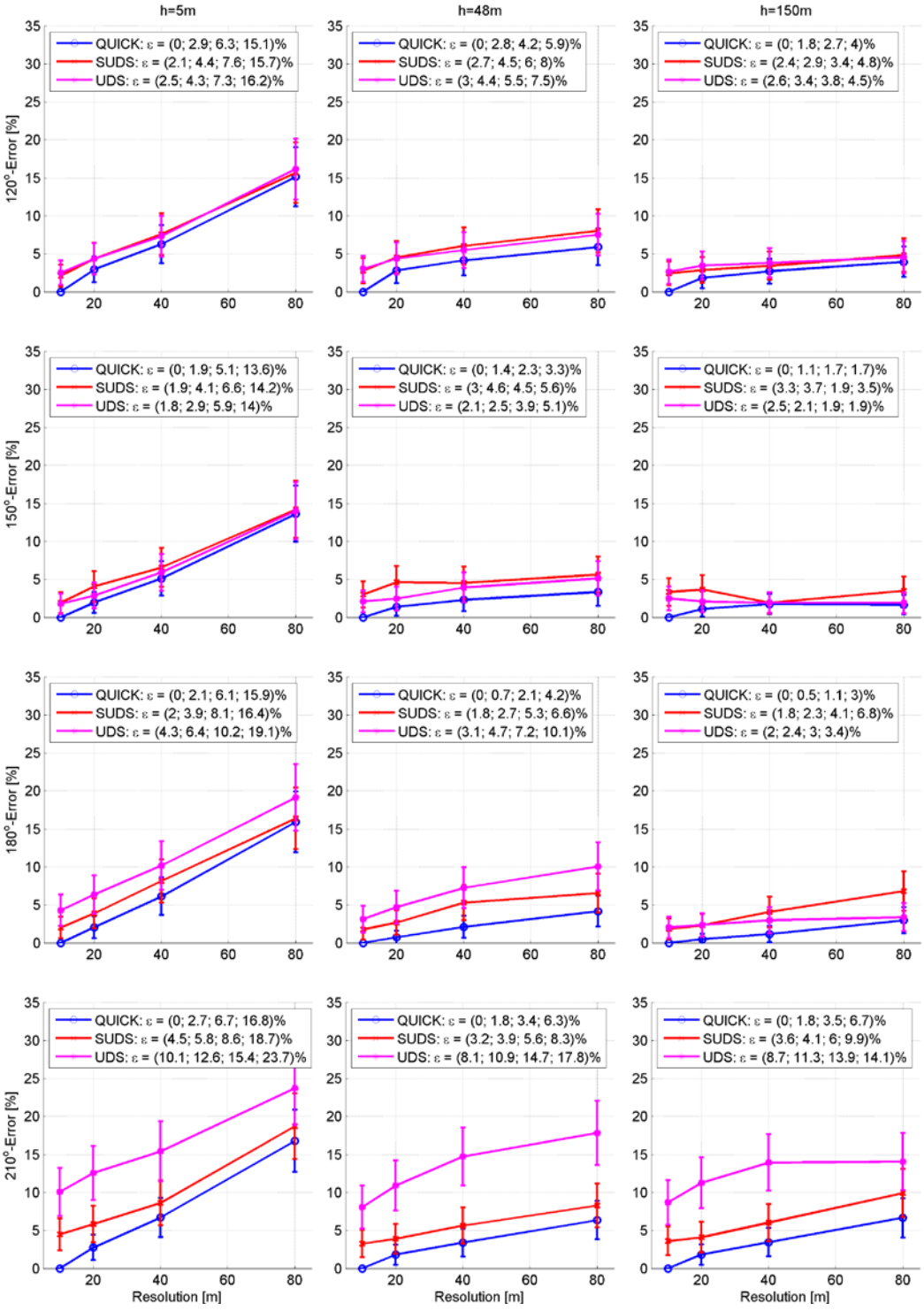

Mean Speed error in the target area for the 120-210 degree wind direction

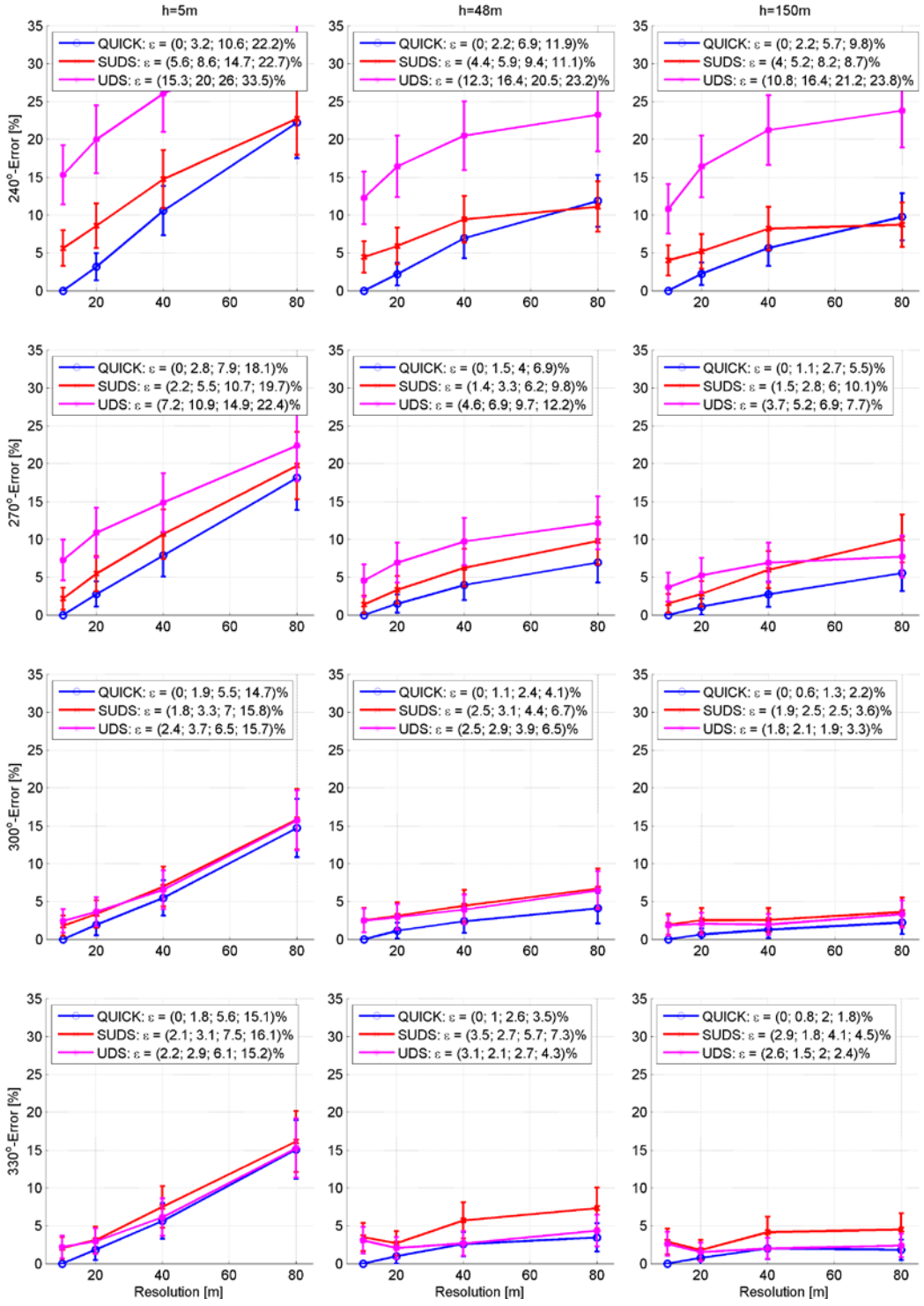

Mean Speed error in the target area for the 0-90 degree wind direction

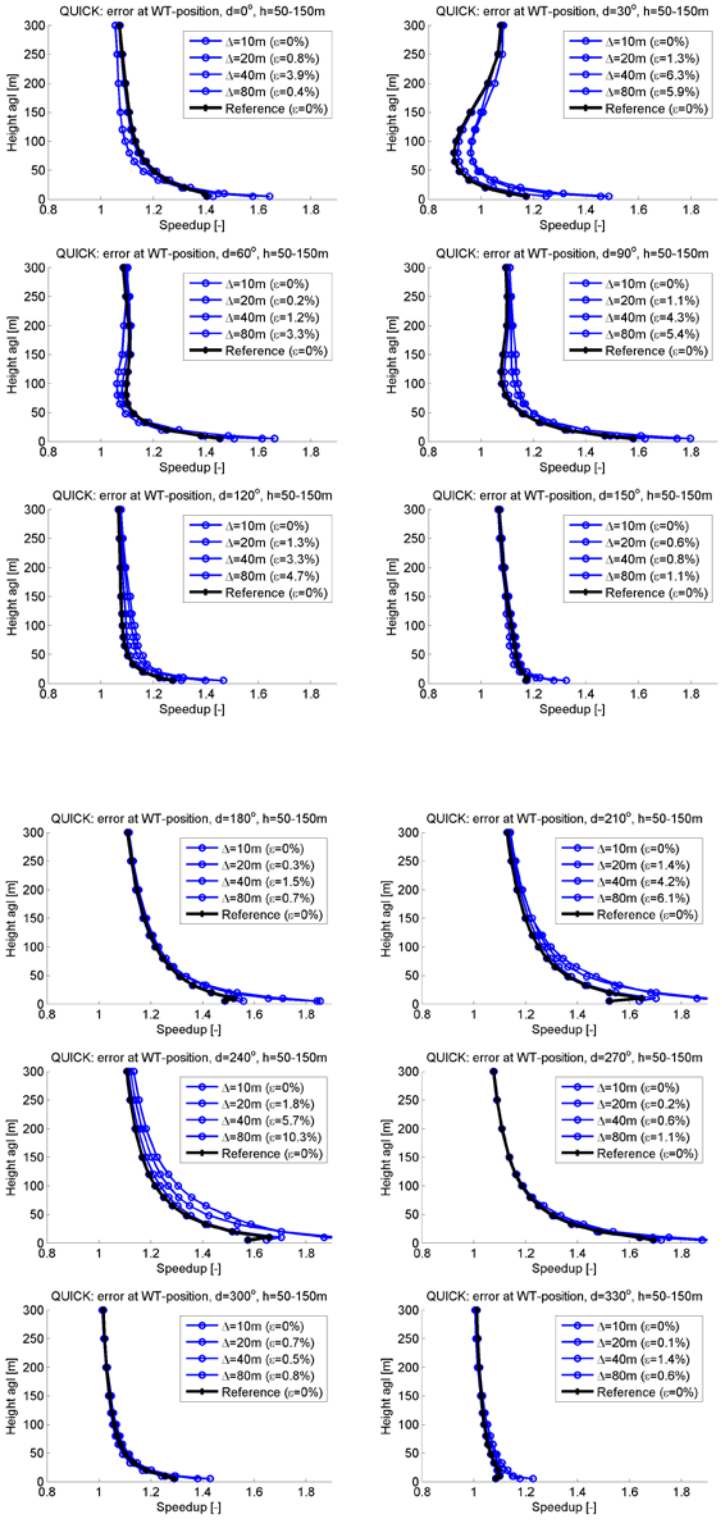

Speed error at WT-position for QUICK scheme

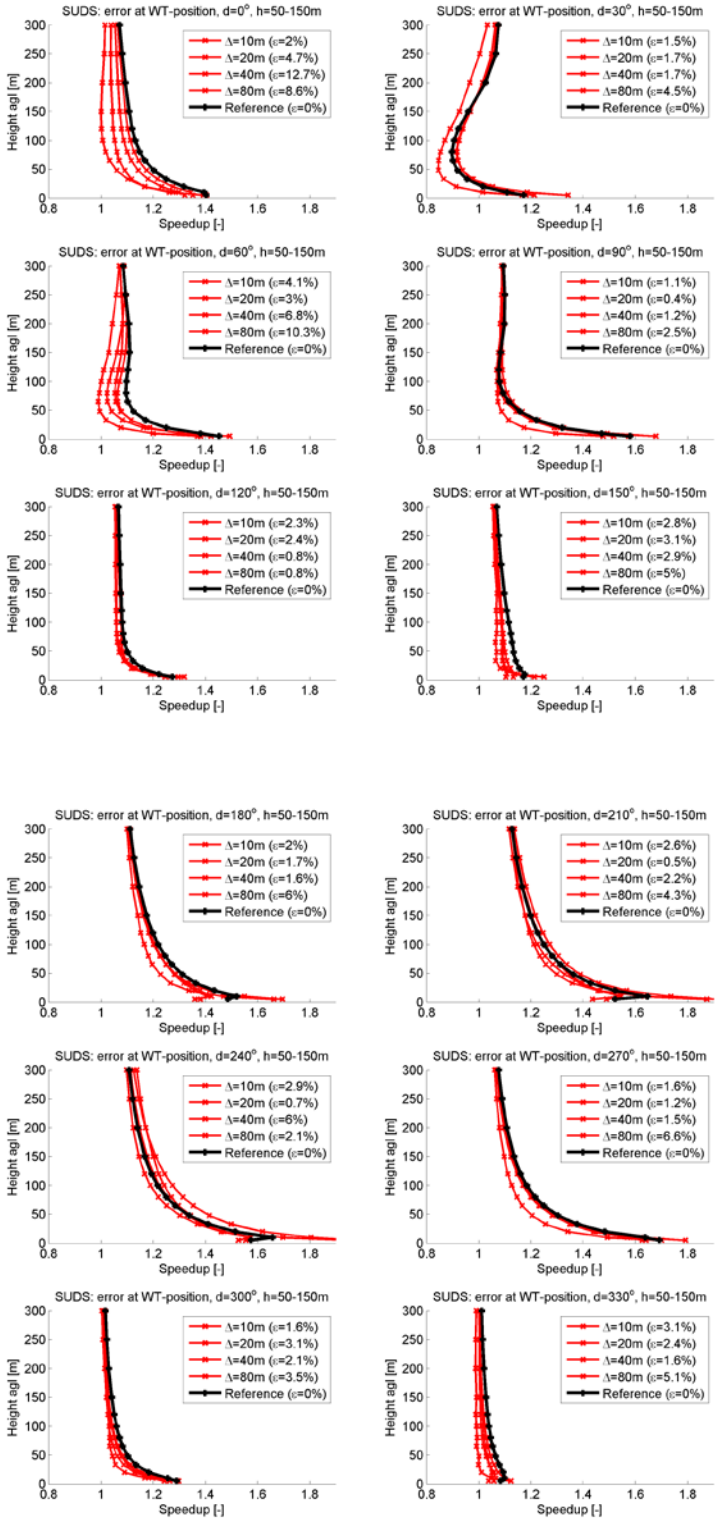

Speed error at WT-position for SUDS scheme

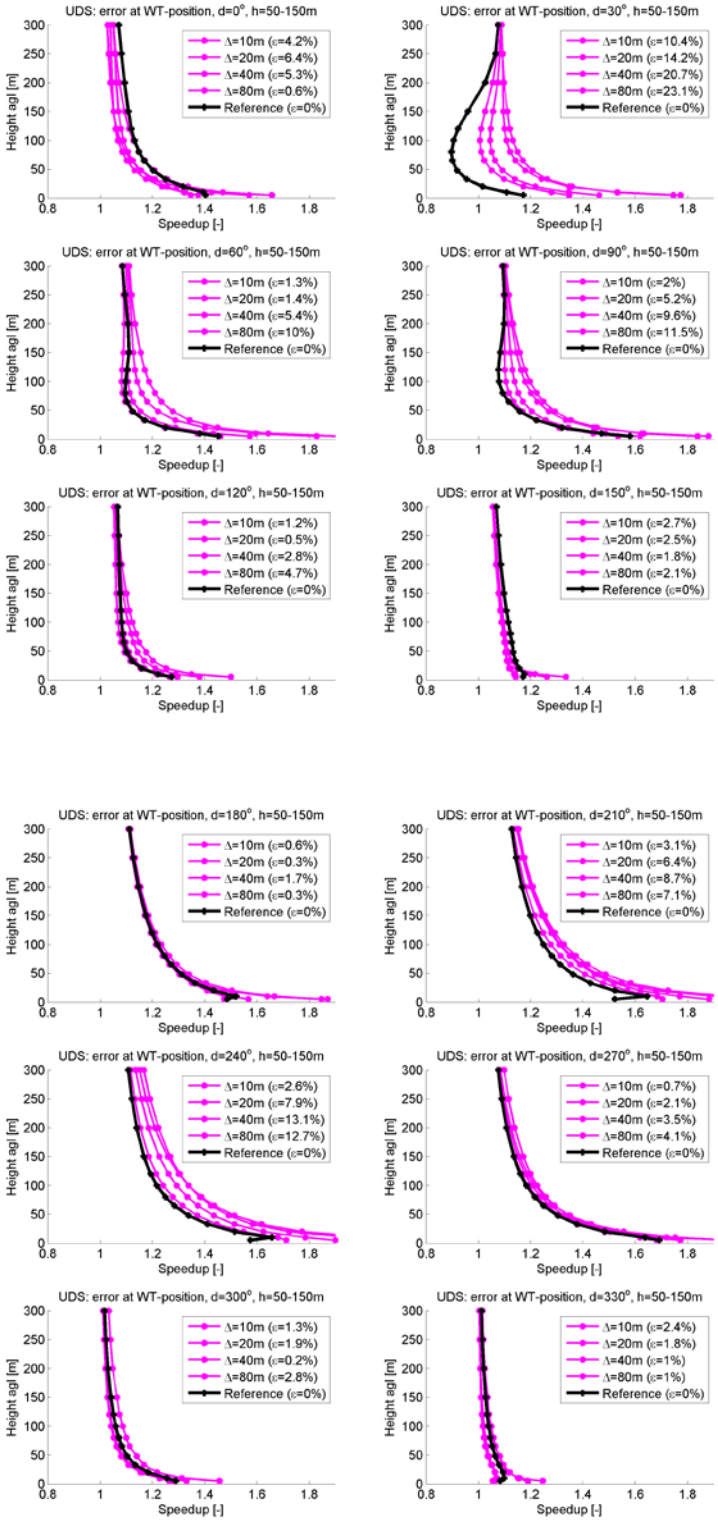

Speed error at WT-position for UDS scheme

DTU Vindenergi er et institut under Danmarks Tekniske Universitet med en unik integration af forskning, uddannelse, innovation og offentlige/private konsulentopgaver inden for vindenergi. Vores aktiviteter bidrager til nye muligheder og teknologier inden for udnyttelse af vindenergi, både globalt og nationalt. Forskningen har fokus på specifikke tekniske og videnskabelige områder, der er centrale for udvikling, innovation og brug af vindenergi, og som danner grundlaget for højt kvalificerede uddannelser på universitetet.

Vi har mere end 240 ansatte og heraf er ca. 60 ph.d. studerende. Forskningen tager udgangspunkt i ni forskningsprogrammer, der er organiseret i tre hovedgrupper: vindenergisystemer, vindmølleteknologi og grundlag for vindenergi.

Danmarks Tekniske Universitet
DTU Vindenergi
Nils Koppels Allé
Bygning 403
2800 Kgs. Lyngby
Telefon 45 25 25 25

info@vindenergi.dtu.dk
www.vindenergi.dtu.dk